Inorganic Chemistry

Article

pubs.acs.org/IC

Six-Coordinate Nitrito and Nitrato Complexes of Manganese Porphyrin

T. S. Kurtikyan,*[,†] V. A. Hayrapetyan,[†] M. M. Mehrabyan,[†] and P. C. Ford*[,‡]

[†]Molecule Structure Research Centre (MSRC) of the Scientific and Technological Centre of Organic and Pharmaceutical Chemistry NAS, 375014, Yerevan, Armenia

[‡]Department of Chemistry and Biochemistry, University of California, Santa Barbara, Santa Barbara California 93106-9510, United States

Supporting Information

ABSTRACT: Reaction of small increments of NO_2 gas with sublimed amorphous layers of $Mn^{II}(TPP)$ (TPP = *meso*-tetraphenylporphyrinato dianion) in a vacuum cryostat leads to formation of the 5-coordinate monodentate nitrato complex $Mn^{III}(TPP)(\eta^1\text{-}ONO_2)$ (**II**). This transformation proceeds through the two distinct steps with initial formation of the five coordinate O-nitrito complex $Mn^{III}(TPP)(\eta^1\text{-}ONO)$ (**I**) as demonstrated by the electronic absorption spectra and by FTIR spectra using differently labeled nitrogen dioxide. A plausible mechanism for the second stage of reaction is offered based on the spectral changes observed upon subsequent interaction of $^{15}NO_2$ and NO_2 with the layered Mn(TPP). Low-temperature interaction of **I** and **II** with the vapors of various ligands L (L = O-, S-, and N-donors) leads to formation of the 6-coordinate O-nitrito $Mn^{III}(TPP)(L)(\eta^1\text{-}ONO)$ and monodentate nitrato $Mn^{III}(TPP)(L)(\eta^1\text{-}ONO_2)$ complexes, respectively. Formation of the 6-coordinate O-nitrito complex is accompanied by the shifts of the ν(N═O) band to lower frequency and of the ν(N−O) band to higher frequency. The frequency difference between these bands $\Delta\nu = \nu(N{=}O) - \nu(N{-}O)$ is a function of L and is smaller for the stronger bases. Reaction of excess NH_3 with **I** leads to formation of $Mn(TPP)(NH_3)(\eta^1\text{-}ONO)$ and of the cation $[Mn(TPP)(NH_3)_2]^+$ plus ionic nitrite. The nitrito complexes are relatively unstable, but several of the nitrato species can be observed in the solid state at room temperature. For example, the tetrahydrofuran complex $Mn(TPP)(THF)(\eta^1\text{-}ONO_2)$ is stable in the presence of THF vapors (∼5 mm), but it loses this ligand upon high vacuum pumping at RT. When L = dimethylsulfide (DMS), the nitrato complex is stable only to ∼−30 °C. Reactions of **II** with the N-donor ligands NH_3, pyridine, or 1-methylimidazole are more complex. With these ligands, the nitrato complexes $Mn^{III}(TPP)(L)(\eta^1\text{-}ONO_2)$ and the cationic complexes $[Mn(TPP)(L)_2]^+$ coexist in the layer at room temperature, the latter formed as a result of NO_3^- displacement when L is in excess.

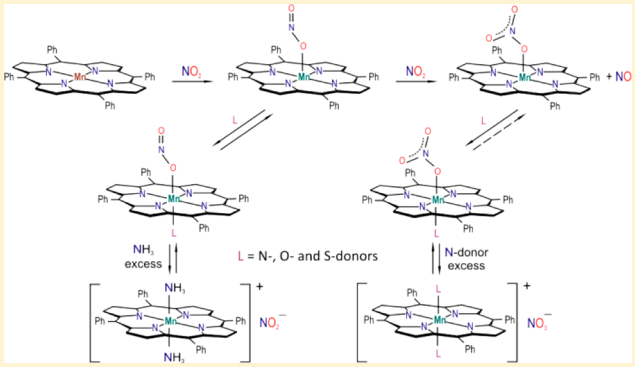

INTRODUCTION

Much of the physiological chemistry of the ubiquitous bioregulator nitric oxide (NO) and other nitrogen oxides is mediated by interactions of these species with metal centers, especially metalloporphyrins. For example, the protective effects of the nitrite anion (NO_2^-) during incidents of hypoxic ischemia[1] has been attributed to its reduction by mammalian heme proteins to generate NO.[2] Nitrite can also be reduced by nitrite reductase (NiR) enzymes, many of which are heme proteins.[2c] In these contexts, we have proceeded to evaluate the interactions of various NO_x species with sublimed layers of various metalloporphyrins in vacuum cryostats where the conditions (including T) can be precisely controlled to map relevant reactivities. Described here are such studies of the nitrito and nitrato complexes of *meso*-tetra-phenylporphyrin-manganese.

The ambidentate nitrite ion can coordinate to metals either at the oxygen to give O-nitrito (M-ONO) or at the nitrogen to give N-nitrito (M-NO_2, often called "nitro") complexes. To our knowledge, a third potential coordination mode involving bidentate binding of both oxygens to the metal is unknown for metalloporphyrins and related metalloproteins. DFT calculations show that energy differences between O-nitrito and N-nitrito structures are small,[3] and there is evidence that the presence and nature of the ligand trans to the nitrite affects the relative stabilities of these linkage isomers. For example, the five-coordinate species $Fe^{III}(Por)(ONO)$ (Por = *meso*-tetraphenyl- or *meso*-tetra-*p*-tolyl-porphyrinato dianions, TPP^{2-} or TTP^{2-}) has O-nitrito coordination,[4a] but once the proximal ligand NH_3 is added, the N-nitrito isomer $Fe(Por)(NH_3)(NO_2)$ is the more stable coordination complex.[4b]

For heme models and proteins, the most common is the N-nitrito coordination mode. The crystal structures for NO_2^-

Received: June 19, 2014
Published: November 4, 2014

   dx.doi.org/10.1021/ic5014329 | *Inorg. Chem.* 2014, 53, 11948−11959

complexes of several ferriheme NiR proteins demonstrate N-coordination.[5] However, there are several published structures of heme proteins with O-bound nitrito coordination.[6] Richter-Addo and co-workers have determined crystal structures of nitrite ion complexes for the ferric forms of myoglobin and hemoglobin (metMb and metHb, respectively) and found both to be O-nitrito species.[6] In this structure, the coordinated oxygen atom of nitrite forms a hydrogen bond with the NH group of histidine imidazole that stabilize O-nitrito coordination. Sustaining this suggestion, the H64 V mutant of metMb, which has the distal histidine replaced by a valine, binds NO_2^- as a N-nitrito complex.[7]

In analogy to the Fe(Por)(ONO) species, O-nitrito coordination is characteristic of the 5-coordinate Mn^{III}(TPP)(ONO) complex (**I**).[8] The crystal structure of the 6-coordinate manganese substituted met-myoglobin Mn(III)Mb(ONO) also reveals the O-bound nitrito coordination,[9] with the structural data also indicating hydrogen-bonding between distal His64 and coordinated oxygen atom of nitrite. However, to our knowledge, the 6-coordinate nitrite complexes of other Mn-porphyrin models have not been characterized. In this context, we describe here the use of sublimed porous layers of **I** as a synthetic precursor to the 6-coordinate complexes with various proximal ligands and use in situ spectroscopy to determine effect on the coordination mode of the nitrite ligand.

Nitrate complexes of metalloporphyrins are involved in key processes in nitrogen cycle and are likely transients formed as the result of heme mediated nitric oxide dioxygenation (NOD)[10] However, examples of 6-coordinate metalloporphyrin complexes of NO_3^- remain relatively rare. These include the trans aqua complex Fe(Por)(H_2O)(η^1-ONO_2) (Por not specified) described in a review,[11] the metastable nitrosyl and tetrahydrofuran species Fe(Por)(L)(η^1-ONO_2) (Por = TPP or TTP; L =NO, THF)[12a,b] obtained by the interaction of NO or THF with thin layers of the Fe(Por)(η^2-O_2NO) and the trans ammine species Fe(Por)(NH_3)(η^1-ONO_2) obtained by reaction of NO with the dioxygen complex Fe(Por)(NH_3)(O_2).[10d] Recently, the 6-coordinate nitrato-complexes Co(Por)(L)(η^1-ONO_2) (Por = TPP or TTP, L = NH_3 or pyridine (Py)) were demonstrated to result from NOD mediated by Co-porphyrins.[13] These also proved to be thermally unstable and decomposed at temperatures above 210 K. However, to our knowledge there have been no reports of stable, 6-coordinate nitrato complexes of the manganese porphyrins.[14] We also describe here the formation and reactivities of such species.

EXPERIMENTAL SECTION

The manganese(II) porphyrinates Mn(Por) are very sensitive to oxygen and are readily oxidized. For this reason the more stable penta-coordinate complexes Mn(TPP)(B) with nitrogen bases (B is Py or piperidine) were used as the precursors to prepare sublimed layers. The complexes Mn(TPP)(B) were synthesized according to published methods.[15]

The low-temperature sublimate was prepared by placing a Mn^{II}(TPP)(B) sample in a Knudsen cell and heating to about 470 K under high vacuum ($P = 3 \times 10^{-5}$ Torr). Evacuation for 2 h resulted in the elimination of the axial ligands B, as monitored by measurement of the pressure at the cryostat outlet. Liquid nitrogen was then poured into the cryostat, and the Knudsen cell was heated to 510 K, at which temperature sublimation of Mn(TPP) onto the surface of the low-temperature (77 K) substrate (KBr or CaF_2) occurred. In the latter case, CaF_2 plates were also used as the optical windows of the cryostat. The metal tetra-arylporphyrin layers obtained in this manner are sponge-like and have high microporosity;[16] thus, potential reactants easily diffuse across these layers, and adducts thus formed can be studied spectroscopically without solvent interference.

Sublimation was typically carried out over periods of 0.5−2.0 h to build up layers of thickness sufficient for UV−visible and IR spectral studies. The substrate with the Mn(TPP) sublimed layers was then heated to room temperature under dynamic vacuum, after which small increments of NO_2 gas were introduced for a short time period followed by a period of pumping out. This procedure led initially to formation of the O-nitrito species Mn(TPP)(η^1-ONO) (**I**) that is oxidized to the nitrato complex Mn(TPP)(η^1-ONO_2) (**II**) after adding more NO_2.[17] FTIR and UV−visible spectra were measured after each NO_2 introduction to ensure formation of **I** and **II**. After this was accomplished, a volatile ligand (NH_3, Py, 1-methylimidazole (1-MeIm), THF or DMS) was fed to the cryostat containing cooled by LN_2 layers of **I** or **II** and the FTIR or electronic absorption spectra were measured in the course of slow warming.

For solution experiments the thermally stable 6-coordinate complexes were scraped from the surface of the KBr substrate and put on the bottom of the flask fitted with an adapter, which allowed for syringe access and protected from air with a rubber septum. The small quantity of degassed CCl_4 was transferred to this flask using a vacuum line and LN_2. The solution prepared in this way was sampled with a Hamilton gastight syringe and injected into the 0.6 mm IR cell through the septum. FTIR spectra were measured using the spectrum of CCl_4 as a background.

NO_2 ($^{15}NO_2$), obtained by oxidation of NO (^{15}NO) with excess of pure dioxygen, was dried over P_2O_5 and then was purified by fractional distillation until a pure white solid was obtained. For isotopic experiments, ^{15}NO with 98.5% enrichment was purchased from the Institute of Isotopes, Republic of Georgia. $N^{18}O_2$ ($^{15}N^{18}O_2$) was synthesized according to the following procedure. The 1:2 mixture of N_2 ($^{15}N_2$) and $^{18}O_2$ gases (Cambridge Isotopic Laboratories) was introduced into an evacuated glass balloon provided with inserted electrodes. Upon continuous electric discharge the colorless gas mixture turned to reddish-brown indicating the formation of $N^{18}O_2$ ($^{15}N^{18}O_2$).

FTIR spectra were recorded using a "Nexus" spectrometer from Thermo Nicolet Corporation and UV−visible spectra on a Specord M-40 spectrophotometer.

RESULTS AND DISCUSSION

Reaction of Nitrogen Dioxide Gas with Solid Mn^{II}(TPP). Studies by Kurtikyan et al.[17] have shown that the reaction of NO_2 with amorphous layers of Mn(TPP) eventually leads to formation of the nitrate analog Mn(TPP)(η^1-ONO_2) (**II**), which was characterized spectroscopically in these layers. **II** had previously been prepared and structurally characterized by Suslick and Watson[8] via the reaction of Mn(TPP)(Cl) with aqueous $Ag(NO_3)$ in a biphasic CH_2Cl_2/H_2O reaction mixture. The formation of insoluble AgCl effectively removed Cl^- from the reaction mixture, allowing the weaker binding NO_3^- to coordinate. The X-ray structure of the Mn(TPP)(NO_3).$2C_6H_6$ crystals showed monodentate coordination of nitrate.

It will be shown here that the reaction of NO_2 gas with amorphous layers of Mn(TPP) proceeds via two distinct stages. At low NO_2 pressures and short contact time, new IR bands in the vicinity of 1445 and 1040 cm^{-1} grow in intensity (Figure 1). In these spectral ranges the porphyrin itself has intense bands, and in amorphous layers the bands of the new species are not distinctly resolved. However, when the $^{15}NO_2$, $N^{18}O_2$, and $^{15}N^{18}O_2$ isotopomers are used, the high frequency band in the vicinity of 1450 cm^{-1} shifts to 1420, 1410, and 1384 cm^{-1}, respectively, and are clearly seen (see Supporting Information Figure S1 the spectrum of Mn(TPP)($^{18}O^{15}N^{18}O$)). The band at about 1040 cm^{-1} also undergoes low-frequency shift, but overlap with an intense porphyrin band near 1000 cm^{-1} prevents determining its frequency distinctly. These bands

dx.doi.org/10.1021/ic5014329 | Inorg. Chem. 2014, 53, 11948−11959

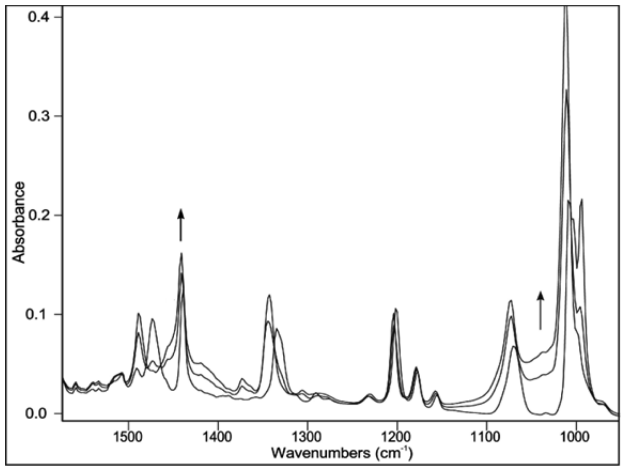

Figure 1. Formation of Mn-porphyrin O-nitrito complex **I** upon reaction of small NO_2 increments (~0,1 Torr) with amorphous layer of Mn(TPP).

appear at frequencies corresponding to ν(N=O) and ν(O−N) of coordinated O-nitrito group,[18] as was seen in the IR spectrum of crystalline **I** at 1444 and 1029 cm^{-1},[8] the X-ray structure of which reveals O-coordination.[8] Thus, we conclude that the first species formed in this reaction is the O-nitrito complex (**I**). Consistent with this assignment, the electronic absorption spectrum of this layered species (Figure 2, dashed line) is similar to that of **I** in benzene solution.[8]

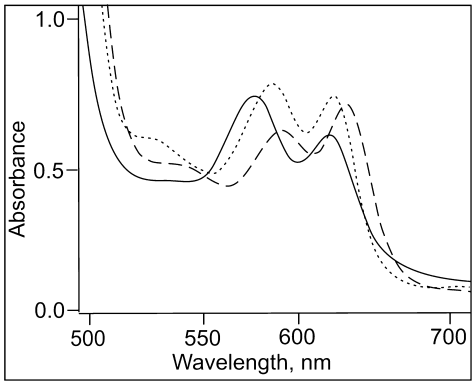

Figure 2. Electronic absorption spectra of layered Mn(TPP) (solid), **I** (dashed), and **II** (dotted line).

It should be noted that the formation of **I** is accompanied by the considerable other changes in the vibrational spectrum. Most of bands attributed to porphyrin ring vibrations[19] undergo shifts to higher frequency (See Supporting Information Figure S2), thus the shifting of these bands shows that none of the initial Mn^{II}(TPP) remains in the layer at this stage of reaction. Especially useful for this purpose is the band corresponding to a porphyrin core deformational mode at 427 cm^{-1} that shifts to 455 cm^{-1} upon formation of **I**.

Supplying additional NO_2 portions into the cryostat leads to the FTIR spectral changes represented in Figure 3. The nitrite band in the vicinity of 1040 cm^{-1} disappears and new intense bands appear at 1470 and 1284 cm^{-1}. These bands underwent expected shifts when labeled the nitrogen dioxides $^{15}NO_2$, $N^{18}O_2$, and $^{15}N^{18}O_2$ were used. (Supporting Information, Figure S3 for ^{15}N-containing species). The data summarized in Table 1 and clearly indicate formation of the nitrato complex **II**.

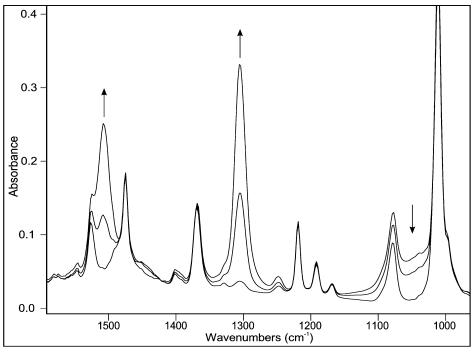

Figure 3. FTIR spectral changes resulting from stepwise addition of NO_2 increments ($P \approx 0.3$ Torr, 2−3 min exposure) to Mn(TPP)(ONO) in sublimed layers and evacuation after each step.

Table 1. IR Frequencies in cm^{-1} of Differently Labeled Nitrato Group Coordinated in Monodentate Fashion in 5-Coordinate Complexes of Metalloporphyrins

adduct	$\nu_a(NO_2)$	$\nu_s(NO_2)$	ν(O−N)	Q bands	ref
Mn(TPP)(η^1-ONO_2)·$2C_6H_6$ crystalline	1474	1286			8
Mn(TPP)(η^1-ONO_2) amorphous	1470	1284	998	580, 615	17
Mn(TPP)(η^1-$O^{15}NO_2$)	1433	1261	985		this work
Mn(TPP)(η^1-$^{18}ON^{18}O_2$)	1448	1258	959		this work
Mn(TPP)(η^1-$^{18}O^{15}N^{18}O_2$)	1412	1228	957		this work
Fe(OEP)(η^1-ONO_2)	1515	1276	980		12b

Notably, the electronic spectrum of this new species (Figure 2) is very close to that reported for **II** in benzene solution.[8]

In these compounds, the nitrate ion is O-coordinated in monodentate fashion.[8] The three IR-active stretching modes expected for this structure would be a low-frequency ν(O−N) band for the coordinated oxygen and two (symmetric and asymmetric) modes for the uncoordinated NO_2 fragment. Three bands at 1474, 1385, and 1286 cm^{-1} were reported in the IR spectrum of crystalline **II** taken in KBr pellets.[8] The frequencies of the first and third bands are very close to those seen in the amorphous layers, the minor frequency differences easily explained by crystal packing effects. The band at 1385 cm^{-1} is absent in our spectra. However, as demonstrated earlier for **II**[8] and also for Fe(OEP)(η^1-ONO_2),[12b] this discrepancy is due to ion exchange (eq 1) that occurs upon grinding nitrato complexes together with KBr. The band at 1385 cm^{-1} can be attributed to the degenerate ν_3(E) vibration of the free nitrate anion.

$$Mn^{III}(TPP)(\eta^1\text{-}ONO_2) + KBr \rightarrow Mn^{III}(TPP)(Br) + KNO_3 \quad (1)$$

By analogy with other nitrato complexes[18] the bands at 1470 and 1284 cm^{-1} can be assigned to the $\nu_a(NO_2)$ and $\nu_s(NO_2)$ vibrations of the uncoordinated NO_2 fragment. Hence the third band belonging to the ν(O−N) stretching for the coordinated oxygen usually disposed in the range of 1000 cm^{-1}[18] is most likely masked by the intense porphyrin band in this range. This band is indeed apparent at 959 cm^{-1} in the spectra of species containing the ^{18}O labeled nitrato group (Table 1, Figure 4, solid line). From Figure 4 it is also clear that this band has low

dx.doi.org/10.1021/ic5014329 | Inorg. Chem. 2014, 53, 11948−11959

intensity and readily can be obscured in the unlabeled nitrate complex by the intense porphyrin band.

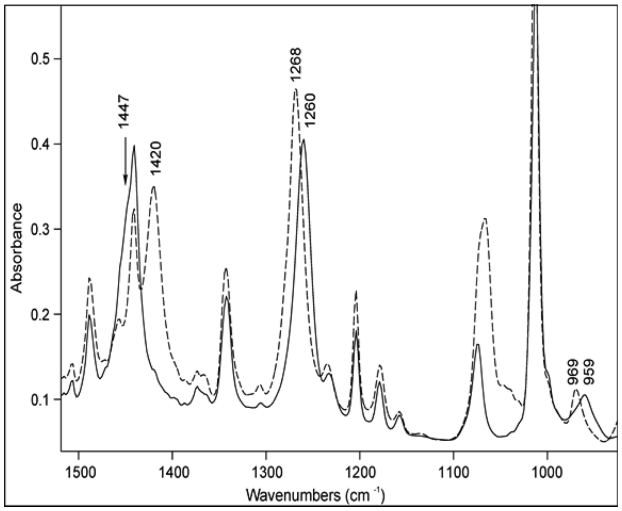

Figure 4. FTIR spectra of Mn(TPP)(η^1-$^{18}ON^{18}O_2$) (solid line) and of Mn(TPP)(THF)(η^1-$^{18}ON^{18}O_2$) (dashed line).

The IR bands of porphyrin core are at the same positions for the η^1-nitrito and nitrato species but are shifted from those of Mn^{II}(TPP). The latter species has a high-spin d^5 configuration and an ionic radius too large to form a planar porphyrinato complex.[20] While the Mn^{III} nitrito and nitrato complexes are also high-spin,[8] they have the d^4 configuration and the vacancy in the $d_{x^2-y^2}$ orbital allows the metal to sit closer to the plane of porphyrin. This changes the overlap of the manganese d_π orbitals with the porphyrin $e_g(\pi^*)$ orbitals resulting in changes in the porphyrin ring vibrations.

From these data, it is clear that the formation of nitrato complex in the course of NO_2 reaction with Mn^{II}(TPP) proceeds via 2 stages. During the first, which is seen for short reaction times with a very low P_{NO_2}, simple NO_2 coordination gives the 5-coordinate O-nitrito complex Mn^{III}(TPP)(η^1-ONO). The formation of **I** upon reaction of low concentration NO_2 gas with the solid Mn(TPP) was also reported by Suslick and Watson.[8] Subsequent reaction at higher P_{NO_2} leads to the slower formation of the nitrato species **II**, presumably with the concomitant formation of NO (Scheme 1). The latter step draws support from the observation that when, at the conclusion of this procedure, the gaseous contents were frozen onto the cryostat wall with LN_2, a bluish solid was observed. This is a qualitative indication of the presence of N_2O_3 formed by reaction of NO with excess NO_2.

The analogous NO_2 reaction with Fe(TPP) also results in formation of a nitrato complex[21] but in that case, nitrate coordination is bidentate, Fe(TPP)(η^2-O_2NO).[11] The characteristic differences between IR spectra of mono- and bidentate coordinated nitrato complexes of metalloporphyrins have been described previously.[16c]

Scenarios for the NO_2 Oxidation of I. For conversion of the O-nitrito complex to the O-nitrato analog, two scenarios can be suggested. The first would involve oxygen atom transfer from free NO_2 to the nitrogen of the Mn−O−N═O moiety to give the nitrato analog (Scheme 2, a). The alternative mechanism would involve attack of NO_2 at the coordinated O atom to give a new Mn(η^1-ONO_2) species with simultaneous displacement of NO from the originally coordinated nitrite ion (Scheme 2, b).

These possibilities can be probed by using isotope labeling experiments. If the first scenario were operating, the reaction of NO_2 with the ^{15}N-labeled O-nitrito complex Mn(TPP)(η^1-$O^{15}NO$) should give the labeled nitrato product Mn(TPP)(η^1-$O^{15}NO_2$), while the second scenario should give the unlabeled analog. The results of such a study are demonstrated in the Supporting Information, Figure S4, in which the sequential changes of the FTIR spectra upon addition of new NO_2 increments to layered Mn(TPP)(η^1-$O^{15}NO$) are shown. It is seen from these spectra that this procedure is accompanied mostly by the appearance and growth of bands at 1284 and 1471 cm^{-1} characteristic of Mn(TPP)(η^1-ONO_2) (Table 1). Simultaneously, there was some growth in the band at 1261 cm^{-1} characteristic of Mn(TPP)(η^1-$O^{15}NO_2$), but this was at least an order of magnitude less than that of the 1284 cm^{-1} band.

The experiments with sequential introduction of $^{15}NO_2$ and NO_2 increments to the Mn(TPP) layer gave spectral changes indicating formation primarily of Mn(TPP)(η^1-ONO_2) consistent with the second of these scenarios being dominant. However, if this is so, then why was some of labeled product formed upon sequential additions of $^{15}NO_2$ and NO_2 increments to the Mn(TPP) layer (the first scenario described above). Although, this might indicate a lesser but active role for oxygen atom transfer to the O-coordinated nitrite, we believe the more likely explanation is related to the isotope scrambling reaction shown in eq 2. Once ^{15}NO is released by the attack of NO_2 on Mn(TPP)(η^1−$O^{15}NO$) this should undergo exchange with the free NO_2 present. The resulting $^{15}NO_2$ formed would then give the labeled product upon further reaction with the O-nitrito complex. This isotope-scrambling reaction has been shown to occur in analogous layers at very low temperatures[16c] and should readily proceed at room temperature conditions of the present experiment. Thus, we conclude that NO_2 oxidation of the O-coordinated nitrite is proceeding by attack of NO_2 at the coordinated oxygen of the Mn−$O^{15}NO$ moiety.

$$^{15}NO + NO_2 \rightleftharpoons {}^{15}NO_2 + NO \quad (2)$$

Scheme 1

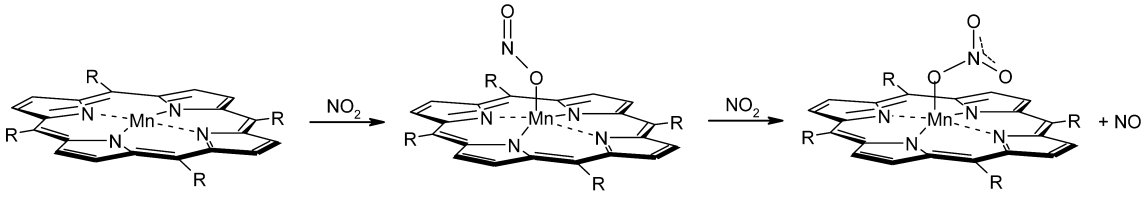

dx.doi.org/10.1021/ic5014329 | Inorg. Chem. 2014, 53, 11948−11959

Scheme 2

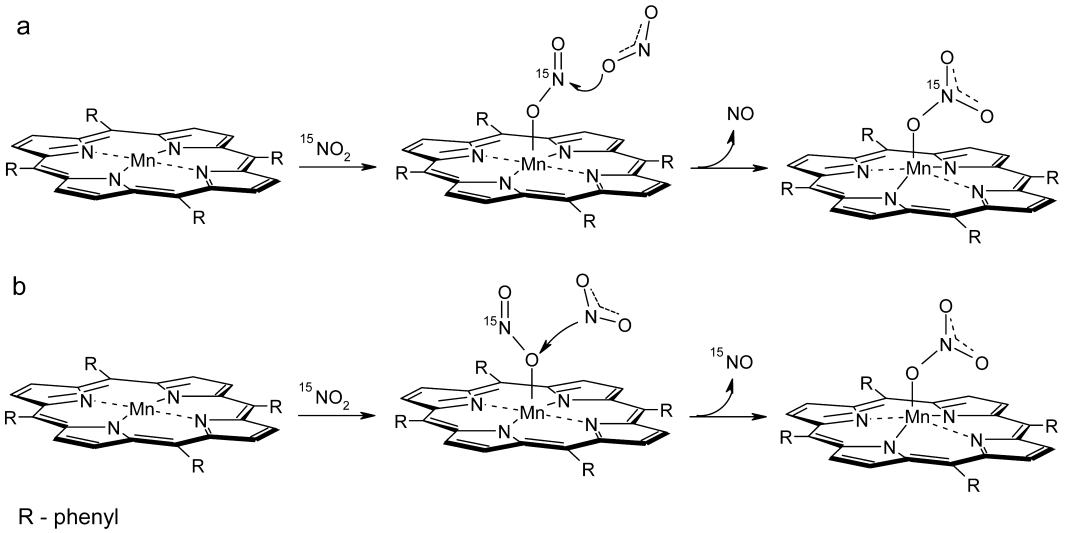

It is, however, noteworthy that above-mentioned isotope labeling experiments can not completely rule out a mechanism that involves homolytic disruption of the $Mn^{III}O-{}^{15}NO$ bond of coordinated nitrito ligand to give a $Mn^{IV}=O$ moiety that then reacts with free NO_2 to give the $Mn(TPP)(\eta^1\text{-}ONO_2)$ end product. For example, this might be facilitated by NO_2 attack at the ^{15}N atom of the nitrito ligand to form $Mn^{IV}=O$ plus dinitrogen trioxide. However, this would appear to be energetically much less likely than the concerted pathway described by the second scenario.

It is worth mentioning that an analogous reaction takes place in the case of iron porphyrins. Interaction of NO_2 with Fe(Por) leads initially to formation of nitrito complex and then to nitrato species.[3c] In contrast the Co-porphyrins reveal different reactivity; after formation of the 5-coordinate N-nitrito-complexes $Co(TPP)(NO_2)$ at low NO_2 pressures, introduction of the new NO_2 increments results in oxidation of porphyrin ring with formation of the π-cation radical.[22]

It will be shown below that the second stage of the reaction represented in Scheme 1 takes place also when nitrito complex is 6-coordinated. As a result, the 6-coordinate nitrato complex formed from the reaction of Mn(TPP)(1-MeIm)(ONO) with NO_2 is fairly stable in the solid state. This observation is of biological significance since in most Mn-substituted heme proteins, the metal is coordinated with the imidazole moiety of a proximal histidine.[9]

Six-Coordinate O-Nitrito Complexes of Mn(TPP). After preparation of the nitrito complex **I** by interaction of small increments of NO_2 with a thin layer of $Mn^{II}(TPP)$ (Figure 1), the sample was cooled with LN_2, and then various ligands in the small quantities controlled with mercury manometer were introduced to the cryostat. The FTIR and UV−visible spectra were measured in the course of slow warming. At various temperatures, at which the ligands gain sufficient mobility to penetrate into the layers, the intensities of the ν(N=O) and ν(N−O) bands of coordinated O-nitrito group in **I** began to decrease, and new bands grew at frequencies disposed at lower than ν(N=O) and higher than ν(N−O) frequencies of **I**. As an example, such spectral changes for L = Py are represented in Figure 5.

The low-frequency shift of ν(N=O) and high-frequency shift of ν(N−O) bands are more clearly seen in the ^{15}N-labeled

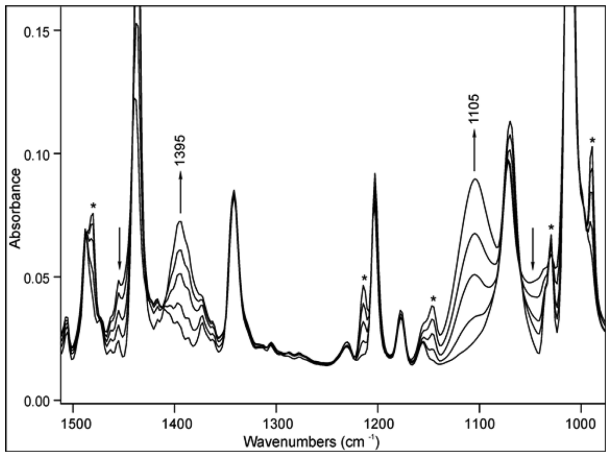

Figure 5. FTIR spectral changes upon introducing 0.3 Torr equivalent of Py into the cryostat containing layered $Mn(TPP)(\eta^1\text{-}ONO)$ and warming slowly from 170 to 210 K. The bands attributed to excess Py are denoted by asterisk.

species. As an example, the spectra of $Mn(TPP)(\eta^1\text{-}O^{15}NO)$ before and after interaction with DMS are represented in Supporting Information, Figure S5. These bands reveal the expected isotopic shifts (Figure 6 for L = Py, Table 2), thus they can unambiguously be assigned to the species containing coordinated nitrite.

As noted above, the nitrite ion can coordinate to metals either at the oxygen (M−ONO) or at the nitrogen ($M-NO_2$). Infrared spectroscopy provides a diagnostic for differentiating between O-nitrito (η^1-ONO) and N-nitrito (η^1-NO_2) coordination.[18] The high frequency stretching modes are much more separated for the O-bound than for the N-bound species. Indeed, for the particular case of metalloporphyrins for the N-nitrito complexes $Fe(TPP)(L)(NO_2)$ (L = N-, S-, and O-donor ligands) the asymmetric $\nu_a(NO_2)$ and symmetric $\nu_s(NO_2)$ modes of coordinated NO_2 are located in the vicinity of 1400 and 1300 cm^{-1}.[4b,23] The same bands of 6-coordinate N-nitrito complexes for Co(TPP) are disposed in the vicinity of 1440 and 1300 cm^{-1} for *trans*-N-, -S-, and -O-donor ligands.[24] The distinctive feature of these bands is much the higher intensity of the lower frequency $\nu_s(NO_2)$ band. Additionally, a fairly intense

dx.doi.org/10.1021/ic5014329 | *Inorg. Chem.* 2014, 53, 11948−11959

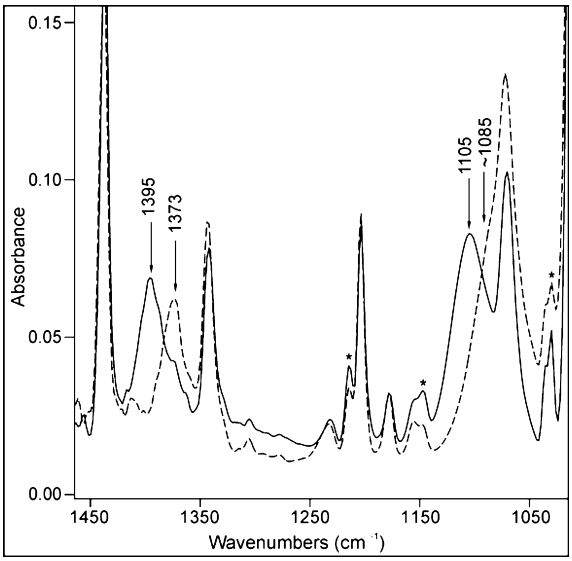

Figure 6. FTIR spectra of the product formed by the reaction of Py with Mn(TPP)(ONO) (solid line) and with Mn(TPP)(O[15]NO) (dashed line) at 210 K. The bands attributed to excess Py are denoted by asterisk.

band for the deformational vibration $\delta(NO_2)$ is disposed in the vicinity of 820 cm^{-1}.

The limited examples of O-nitrito complexes of metalloporphyrins include the 5-coordinate nitrito complexes of iron- and manganese- porphyrins[4,8] and the 6-coordinate nitrito complexes of Fe-porphyrins with *trans*-NO,[3b,4a] -NH_3,[4b] and -THF[23] ligands. The 5-coordinate Fe(Por)(η^1-ONO) (Por = TPP and TTP) complexes displayed IR bands in the vicinity of 1520, 900, and 750 cm^{-1} assigned to ν(N═O), ν(N−O), and δ(ONO) of the O-coordinated nitrito ligand.[4a] These bands shift to about 1470, 970, and 825 cm^{-1} upon formation of the 6-coordinate species Fe(Por)(NH_3)(η^1-ONO) upon reaction of gaseous NH_3 with layered Fe(Por)(η^1-ONO) at low-temperature.[4b] Bands in the range of 1510 and 930 cm^{-1} were reported for the metastable O-nitrito species Fe(TPP)(NO)(η^1-ONO) obtained by photolysis of the N-nitrito complex Fe(TPP)(NO)(NO_2) in a low-temperature KBr pellet,[3b] and also by low-temperature reaction of NO gas with sublimed layers of Fe(Por)(η^1-ONO).[3c] Thus, transition from 5- to 6-coordination is accompanied by the low-frequency shift of ν(N═O) and high-frequency shift of ν(N−O) band. Additionally, in all these cases, the intensities of these bands are close to each other in contrast to the N-nitrito analogs. Based on this spectral analysis, we conclude that the spectral changes observed for the reactions of **I** with various ligands can be interpreted in terms of forming the 6-coordinate O-nitrito Mn(TPP)(L)(η^1-ONO) complexes as represented in Scheme 3.

Scheme 3

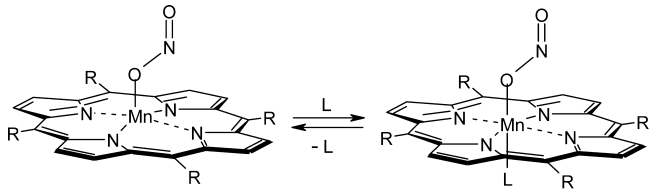

Optical spectra also display changes upon formation of these species. The Q-bands of **I** in the UV−visible spectrum undergo the blue shifts and change their relative intensities upon formation of the 6-coordinate complexes (Figure 7 for the Py derivative, Table 2).

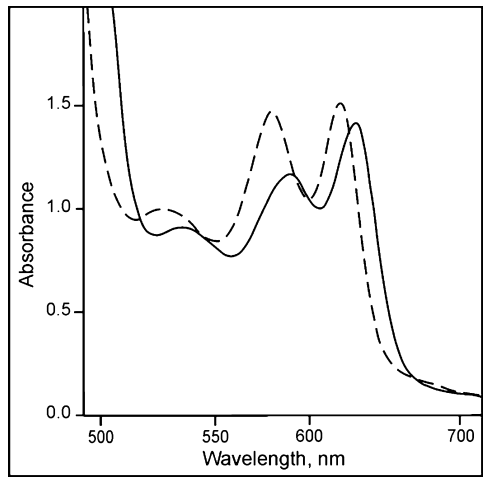

Figure 7. UV−visible spectra of **I** (solid line) and Mn(TPP)(Py)(ONO) (dashed line) at 200 K.

It should be noted here that the above-mentioned 6-coordinate O-nitrito complexes of iron-porphyrins have been

Table 2. Frequencies of Stretching Vibrations (cm^{-1}) for the Coordinated Nitrito Ligand in the 6-Coordinated Complexes of Mn- and Fe-Porphyrins with the Various Electron Donor Ligands[a]

complex	ν(N═O)	ν(N−O)	$\Delta\nu = \nu$(N═O) − ν(N−O)	Q-bands (nm)	ref
Mn(TPP)(η^1-ONO)	1445 (1421)	1040 (~1020)	405 (401)	587, 625	this work
Mn(TPP)(DMS)(η^1-ONO)	1416 (1394)	~1072 (1052)	344 (342)	581, 622	this work
Mn(TPP)(THF)(η^1-ONO)	1415 (1391)	1084 (1055)	331 (336)	577, 616	this work
Mn(TPP)(Py)(η^1-ONO)	1398 (1375)	1105 (1084)	293 (291)	576, 616	this work
Mn(TPP)(NH_3)(η^1-ONO)	1384 (1357)	1115 (1094)	269 (263)		this work
Mn(TPP)(1-MeIm)(η^1-ONO)	1382(1356)	1121 (~1100)	261 (256)	581, 619	this work
Fe(TPP)(η^1-ONO)	1526 (1499)	904 (885)	622 (614)	508,577sh, 659, 689	4a
Fe(TPP)(THF)(η^1-ONO)	1481 (1448)	963 (946)	518 (502)		23a
Fe(TPP)(NH_3)(η^1-ONO)	1475 (1445)	971 (952)	504 (493)	552, 595sh, 650sh, 695sh	4b
Fe(TPP)(NO)(η^1-ONO)	1496 (1471)	938 (920)	558 (551)	548, 574	3c

[a]The data for [15]N-labeled nitrito group are given in the parentheses.

dx.doi.org/10.1021/ic5014329 | *Inorg. Chem.* 2014, 53, 11948−11959

observed only at very low-temperatures. With *trans*-NH_3 and -NO ligands the O-nitrito complexes could be detected at temperatures lower than ~150 K. Further warming led to the isomerization of O-nitrito to N-nitrito coordination. With THF as a trans ligand, both O-nitrito and N-nitrito isomers were present in the narrow temperature interval 130−160 K. Further warming led to elimination THF ligand and restored the 5-coordinate O-nitrito complexes Fe(Por)(η^1-ONO).[23a] In contrast, for the Mn-derivatives there is no spectral evidence indicating a change in the mode of nitrite coordination. Upon temperature increase the only reaction of the 6-coordinate species was dissociation of the proximal ligand to restore the parent O-nitrito complex **I**.

The FTIR data summarized in Table 2 provide the basis for assigning vibrational frequencies for coordinated O-nitrito group for the 6-coordinate nitrite complexes of Mn(TPP), and these assignments are sustained by the data for $^{15}NO_2$ labeled isotopomers. Table 2 also suggests an interesting correlation between the nature of the ligand trans to the O-nitrito group and the difference between the frequencies of ν(N═O) and ν(N−O) vibrational modes $\Delta\nu = \nu$(N═O) − ν(N−O), which follows the order: 1-MeIm < NH_3< Py <THF <DMS. Electronic communication between the axial ligands, L and NO_2, occurs largely through the metal d_{z^2} and d_{xz}, d_{yz} orbitals. In this context, we propose that $\Delta\nu$ is reflective of the net charge transfer to the nitrito group with the smaller $\Delta\nu$ representing more charge transfer. The DMS and THF are weak σ-donor ligands and their influence on the frequencies of ν(N═O) and ν(N−O) stretching modes of **I** is noticeably less than for the stronger N-donor ligands. The latter $\Delta\nu$ does not correlate with the Broensted base strengths of these ligands with 1-MeIm intermediate between Py and NH_3.[25] However, the observed order may be rationalized by taking into account the modest π-donor character of 1-MeIm, while NH_3 is a σ-donor only and Py is a π-acceptor.[26]

Introduction of NH_3 (~0.1 Torr equivalent) to the cryostat containing layered **I** at 120 K followed by slow warming to 170 K led to the FTIR spectral changes represented in Figure 8. The ν(N═O) band of **I** in the vicinity of 1445 cm^{-1} disappears, and new bands in the spectral ranges of 1400, 1230, and 1120 cm^{-1} appear. The bands at 1400 and 1120 cm^{-1} grow with correlating intensities and have their isotopic counterparts seen for the reaction of NH_3 with Mn(TPP)-

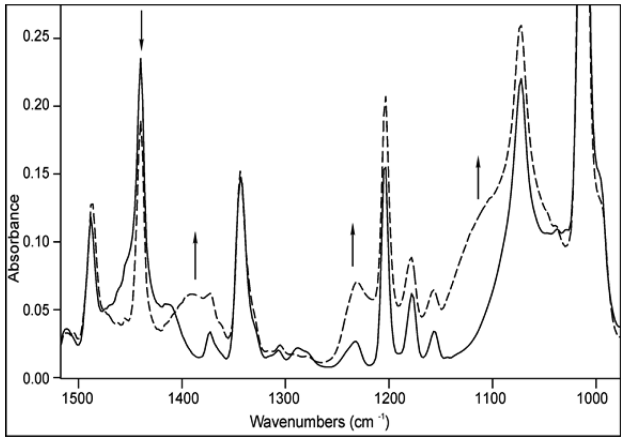

Figure 8. FTIR spectra of **I** (solid line) after supplying the cryostat with ~0.1 Torr equiv NH_3 at 120 K and slow warming to 170 K (dashed line).

(O^{15}NO) (see Table 2). By analogy with the other **I** + L systems they can be assigned to ν(N═O) and ν(O−N) of Mn(TPP)(NH_3)(ONO). The band at 1228 cm^{-1} is also isotope sensitive and greatly enhances in intensity at the expense of the former bands when the higher pressures of NH_3 are supplied in to cryostat as is demonstrated in Figure 9. This

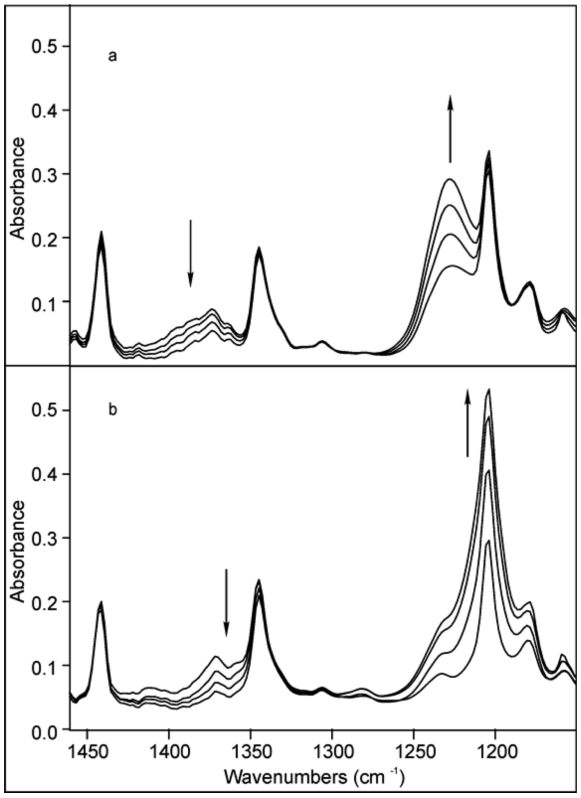

Figure 9. FTIR spectral changes observed upon supplying 3 Torr equivalent NH_3 to the cryostat and warming from 120 to 170 K. (a) Mn(TPP)(ONO) + NH_3 and (b) Mn(TPP)(O^{15}NO) + NH_3.

band is in the spectral range where the $\nu_a(NO_2^-)$ stretching mode of free NO_2^- is disposed.[18] Thus, it appears that nitrite is being displaced by the excess NH_3 with formation of the cationic diammine complex $[Mn(TPP)(NH_3)_2]^+$ plus free NO_2^- as illustrated by Scheme 4.

When the layer is warmed to higher *T*, the intensity of the $\nu_a(NO_2^-)$ band of the free ion begins to decrease with concomitant intensity increase of the bands of Mn(TPP)-(NH_3)(ONO) demonstrating reverse binding of NO_2^- after the loss of one NH_3 from the thermally unstable diammine complex. However, not all the diammine complex is converted back to the mixed six-coordinate species, since some of the latter releases NH_3 to restore the parent O-nitrito complex **I**. These data indicate that complex equilibria depending on the pressure of NH_3 and temperature exists between the species represented on Scheme 4.

None of the 6-coordinate nitrito complexes studied were thermally stable at higher *T*, and each slowly decomposes by losing L upon warming to RT. The adducts with less volatile Py and 1-MeIm ligands are more stable. Pumping overnight leads to complete decomposition of the Py complex while about half of the 1-MeIm complex still is present in the layer after this procedure.

dx.doi.org/10.1021/ic5014329 | *Inorg. Chem.* 2014, 53, 11948−11959

Scheme 4

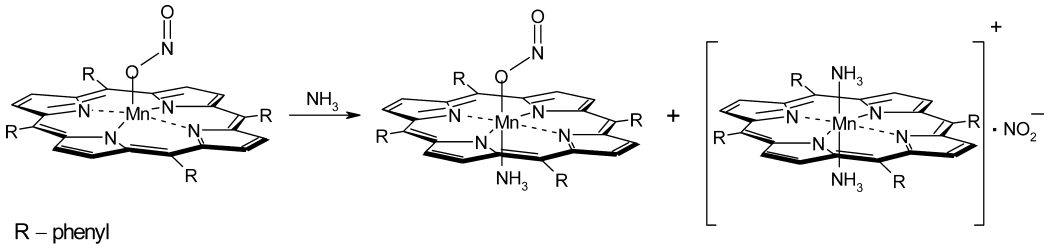

Six-Coordinate Nitrato Complexes of Mn(TPP) with THF and DMS. Introduction of small increments of THF vapor into the cryostat containing thin layers of **II** at LN_2 temperature followed by slow warming leads to shifts of the IR bands of the coordinated nitrato group. The high-frequency $\nu_a(NO_2)$ band shifts noticeably to lower frequency, while the $\nu_s(NO_2)$ band undergoes a minor shift to higher frequency (Figure 10, dashed line). The low-intensity ν(O–N) band also undergoes a shift to higher frequency as seen in Figure 4. The above-mentioned bands show the appropriate isotopic shifts when ^{15}N- or ^{18}O-labeled nitrato complexes were used, confirming their assignment to the coordinated nitrato group (Supporting Information Figure S6, Table 3). These spectral changes are analogous to those observed upon formation of the six-coordinate iron-porphyrins nitrato complex with a *trans*-THF ligand[3b] consistent with formation of the 6-coordinate nitrato-complex Mn(TPP)(THF)(η^1-ONO_2) (Scheme 5). The Q bands in the electronic absorption spectrum shift to higher energy upon coordination to THF (Figure 11).

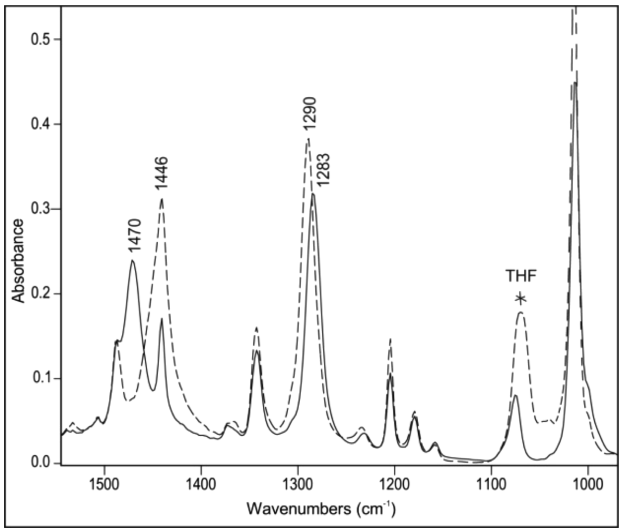

Figure 10. FTIR spectral changes of layered Mn(TPP)(η^1-ONO_2) (solid) upon supplying the cryostat with 0.3 Torr equivalent of THF at LN_2 temperature and slow warming to 180 K. to give Mn(TPP)-(THF)(η^1-ONO_2) (dashed line). The THF excess was mostly pumped out at 180 K.

Scheme 5

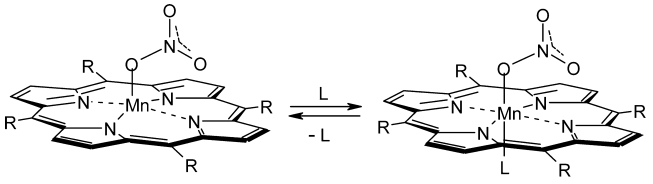

The THF adduct Mn(TPP)(THF)(η^1-ONO_2) can also be obtained at room temperature by exposure of **II** to THF vapor (a few tens of torr). It is stable at room temperature when a few torr of THF are present in cryostat, but it slowly loses the THF ligand in the course of pumping to restore the spectrum of the initial nitrato complex **II**. The THF complex readily decays when it is dissolved in noncoordinating solvent (Supporting Information, Figure S7).

Interaction of the S-donor ligand DMS with **II** leads to the same spectral changes as in the case of THF manifesting the formation of the 6-coordinate complex Mn(TPP)(DMS)(η^1-ONO_2) (Supporting Information, Figure S8). In this case,

Table 3. IR Frequencies (cm^{-1}) of Differently Labeled Nitrato Group in 6-Coordinate Complexes of Metalloporphyrins with the Various Trans Electron Donor Ligands[a]

adduct	$\nu_a(NO_2)$ (cm^{-1})	$\nu_a(NO_2)$	ν(O–N)	Q bands (nm)	refs
Mn(TPP)(DMS)(η^1-ONO_2)	1451 (1407)	1289 (1263)		583, 618	this work
Mn(TPP)(THF)(η^1-ONO_2)	1446 (1410)	1290 (1262)		575, 610	this work
Mn(TPP)(THF)(η^1-$^{18}ON^{18}O_2$)	1419	1269	969		this work
Mn(TPP)(Py)(η^1-ONO_2)	1427 (1393)	1393 (1269)		578, 614	this work
Mn(TPP)(1-MeIm)(η^1-ONO_2)	1418 (1390)	1293 (1264)			this work
Mn(TPP)(NH_3)(η^1-ONO_2)	1426 (1403)	1290 (1260)			this work
Fe(TPP)(NO)(η^1-ONO_2)	1505 (1472)	1265 (1246)	969 (954)	547, 582	12a
Fe(TPP)(THF)(η^1-ONO_2)	1491 (1457)	1280 (1258)	~997 (986)		12b
Fe(TPP)(NH_3)(η^1-ONO_2)	1499 (1472)	1268 (1249)	938 (925)		12
Co(TPP)(NH_3)(η^1-ONO_2)	1484 (1459)	1270 (1248)	983 (970)	558, 597	13a
Co(TPP)(Py)(η^1-ONO_2)	1477 (1449)	1270 (1247)	985 (979)	549	13b

[a]The data for ^{15}N labeled nitrato group are given in parentheses.

dx.doi.org/10.1021/ic5014329 | *Inorg. Chem.* 2014, 53, 11948–11959

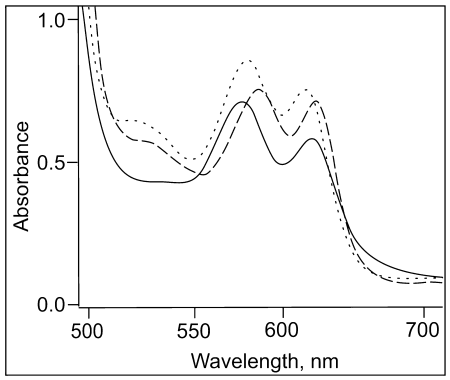

Figure 11. Visible spectra of Mn(TPP) sublimed layer (solid line) after interaction with NO_2 to form **II** (dashed line), then interaction with THF at 180 K (dotted line) (all on a CaF_2 substrate).

however, the complex is less stable and begins to decompose at temperatures above −30 °C (Scheme 5).

Interaction of N-Donor Ligands with II. When small quantity (~0.5 Torr equivalent) of NH_3 was introduced into the cryostat with layered **II** at LN_2, and layer was slowly warmed to 130 K, the FTIR spectral changes shown in Figure 12a were observed. The bands of **II** at 1470 and 1284 cm^{-1} decreased in intensity, and new bands at ~1427 and 1360 cm^{-1} emerged. Their intensities do not correlate, indicating that these new bands belong to different species. From the results described above for the THF and DMS ligands it is reasonable to suggest that the band at ~1427 cm^{-1} is the nitrato $\nu_a(NO_2)$ of $Mn(TPP)(NH_3)(\eta^1\text{-}ONO_2)$ while the shift of the band at 1284 cm^{-1} to higher frequency may involve the overlapping of $\nu_s(NO_2)$ bands of **II** and the 6-coordinate species.

The spectral changes observed upon addition of more NH_3 (1 Torr equivalent) at LN_2 T and warming to 130 K are represented in Figure 12b. The bands of coordinated nitrato group disappear and the broad band near 1360 cm^{-1} and overlapping with the porphyrin band at 1350 cm^{-1} continues to grow. This band has its isotopic analogs in the experiments with ^{15}N-and ^{18}O-containing species and unambiguously can be assigned to the degenerate asymmetric stretching mode $\nu_3(E)$ of the nitrate anion.[18] Consistent with this interpretation a weak, isotopically sensitive band also grows in the vicinity of 830 cm^{-1} where the out-of-plane deformation mode $\nu_2(A_2)$ of NO_3^- anion is disposed (Figure 12b, inset).[18] For this system the doubly degenerate $\nu_3(E)$ band is not a single band but has complex shape (the shoulder at ~1320 cm^{-1} can be noticed in Figure 12b) that is certainly connected with the H-bonding of NO_3^- with NH_3 (coordinated or solvated) that lowers the D_{3h} symmetry of nitrate-anion and removes the degeneracy of $\nu_3(E)$ mode. Such splitting was described in the literature[27] for the NO_3^-/H_2O system. Depending on the quantity of the H_2O molecule per an NO_3^- ion and the symmetry of H-bonding the different characteristics of ν_3 splitting into two components was observed with separation of the bands as much as 43 cm^{-1} in some cases.[27] The same pattern is apparently true for NO_3^-/NH_3. This interpretation gains additional support in the experiments with Py ligand (see below) where the same band manifests itself as a single unperturbed curve.

It can be concluded from this data that when excess NH_3 is present, the nitrate ion can be readily displaced to form the cationic complex $[Mn(TPP)(NH_3)_2]^+$ plus free nitrate anion NO_3^-.

Further warming of this system to room temperature led to partial loss of $[Mn(TPP)(NH_3)_2]^+$ cation accompanied by the reformation of 6-coordinate nitrato-complex $Mn(TPP)(NH_3)(\eta^1\text{-}ONO_2)$ and **II**. Thus, it appears that equilibrium between three different species represented in Scheme 6 is responsible. The relative quantities of these complexes depend on the temperature and NH_3 pressure. Our attempts to find conditions where only the 6-coordinate nitrato-complex was present in layered medium were unsuccessful. The FTIR spectrum of one of such a system is demonstrated in Supporting Information, Figure S9. Although this sample mostly contains the nitrato-ammine complex $Mn(TPP)(NH_3)(\eta^1\text{-}ONO_2)$ (bands at 1427 and 1290 cm^{-1}), there are also noticeable quantities of

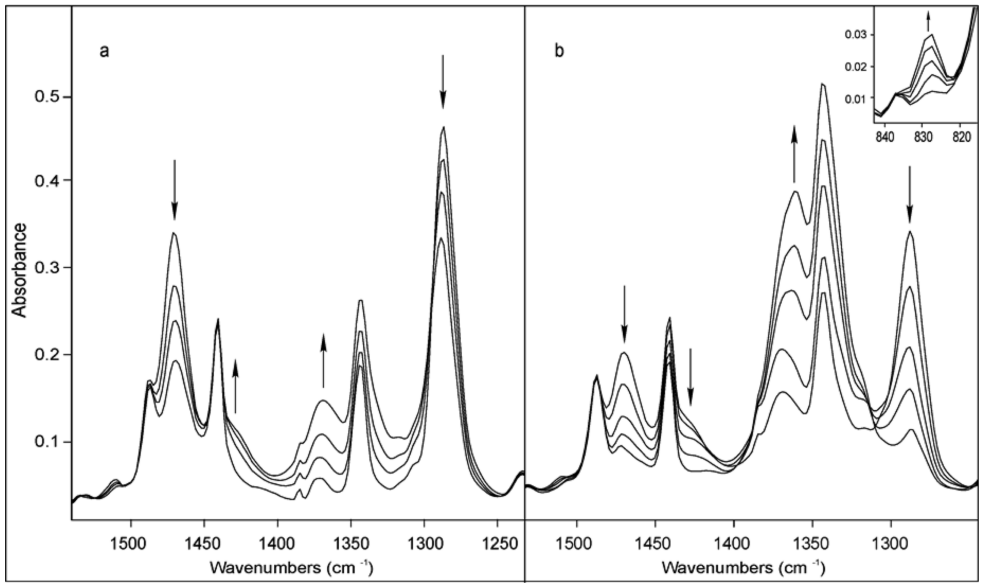

Figure 12. FTIR spectral changes upon supplying (a) 0.5 Torr equivalent NH_3 into layered **II** at LN_2 T and slow warming to 130 K. (b) The same procedure with the additional 1 Torr equivalent NH_3.

dx.doi.org/10.1021/ic5014329 | Inorg. Chem. 2014, 53, 11948−11959

Scheme 6

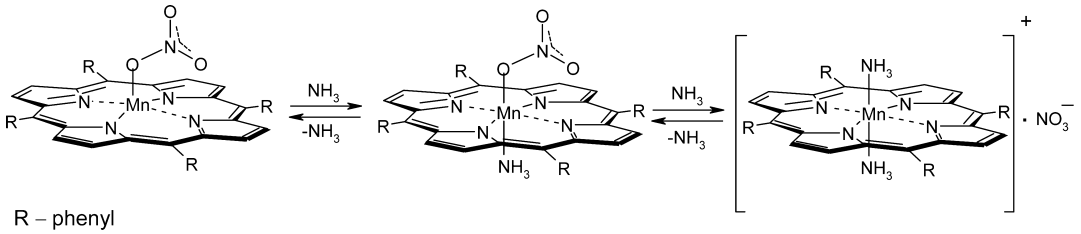

Scheme 7

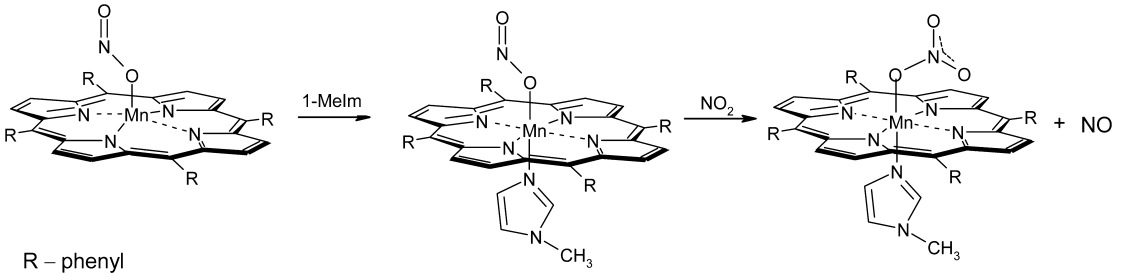

diammonia cationic complex $[Mn(TPP)(NH_3)_2]^+ \cdot NO_3^-$ (band at 1360 cm^{-1}) and **II** (band at 1470 cm^{-1}).

Long-time pumping of the system at RT leads eventually to the complete restoration of **II** demonstrating that neither cationic $[Mn(TPP)(NH_3)_2]^+ \cdot NO_3^-$ nor the nitrato-ammine $Mn(TPP)(NH_3)(\eta^1\text{-}ONO_2)$ complexes are stable in the absence of excess NH_3. Similar behavior was seen for the Fe-porphyrin nitrato complexes.[12b]

Experiments with the less volatile ligand Py gave somewhat different results. Although the presence of excess Py leads to formation of the cationic $Mn(TPP)(Py)_2^+$ and NO_3^- ion, the latter complex could be transformed to the six-coordinate nitrato-pyridyl complex $Mn(TPP)(Py)(\eta^1\text{-}ONO_2)$ by pumping out the cryostat at RT to give the IR spectrum shown in Supporting Information, Figure S10. This result implies that the cationic bis(pyridyl) complex $[Mn(TPP)(Py)_2]^+$ is not very stable at RT.

Another ligand of considerable interest is 1-methyl-imidazole (1-MeIm), which is a mimic of the histidine imidazole in hemeproteins. When layers of **II** in the cryostat were treated with saturated vapors of 1-MeIm, the IR bands of **II** disappeared with the concomitant growth of bands characteristic of a 6-coordinate species. However, a significant quantity of $[Mn(TPP)(1\text{-}MeIm)_2]^+ \cdot NO_3^-$ is also formed. The latter does not transform back to the six-coordinate nitrato complex $Mn(TPP)(1\text{-}MeIm)(\eta^1\text{-}ONO_2)$ upon high-vacuum pumping. Thus, the binding of two axial 1-MeIm ligands in bis-ligated cationic complex is stronger than for Py. The $[Mn(TPP)(1\text{-}MeIm)_2]^+$ complex has been isolated and structurally characterized.[28b]

The strategy demonstrated in Scheme 7 was applied to obtain the 6-coordinate nitrato-complex with a *trans*-1-MeIm ligand (details of experiment and spectral evidence for formation of the $Mn(TPP)(1\text{-}MeIm)(\eta^1\text{-}ONO_2)$ are represented in Supporting Information, Figure S11).

The 6-coordinate nitrato complexes with Py and 1-MeIm are stable in the solid state at RT, but dissolution in non-coordinating solvent leads to their decomposition.

In Table 3 the data on FTIR and UV–vis spectra of six-coordinated nitrato-complexes with the various trans ligands are summarized. As can be seen in all these complexes, the formation of six-coordinate species is accompanied by the lowering of the $\nu_a(NO_2)$ and enhancing of the $\nu_s(NO_2)$ frequencies (compare with the data of Table 1). The magnitudes of these shifts correlate with the donor strengths of the trans ligands: stronger σ-donors result in bigger shifts of these bands from the values of the five-coordinate species. It is noteworthy that a number of 6-coordinate nitrato complexes of Mn(TPP) obtained in this work were thermally stable in the solid state in contrast to the nitrato-complexes of iron and cobalt-porphyrins.[3c,4] Assuming that Mn-porphyrins promotes the NOD-reaction it is reasonable to expect that the resulting species might contain 6-coordinate nitrato-complexes at ambient conditions in contrast to Fe or Co analogs that eliminate the nitrate anion upon warming to RT.

In summary, formation of **II** by interaction of NO_2 gas with amorphous layer of Mn(TPP) proceeds via two distinct stages. At very low P_{NO_2}, NO_2 coordination to give the 5-coordinate O-nitrito complex **I** occurs. Subsequent reaction at higher P_{NO_2} leads to formation of the nitrato complex **II**, with the concomitant formation of NO. A plausible mechanism for this stage of reaction is offered based on the spectral changes observed upon subsequent interaction of $^{15}NO_2$ and NO_2 with the layered Mn(TPP). Reaction of electron donor ligands (L) with **I** leads to formation of the 6-coordinate O-nitrito complexes Mn(TPP)(L)(ONO) that are mostly thermally unstable. Formation of these 6-coordinated complexes is accompanied by the low- and high-frequency shifts of the ν(N=O) and ν(N–O) bands, correspondingly, of the coordinated nitrite. The magnitudes of the shifts depend on the nature of trans ligand and is higher for stronger Lewis base donors. With ammonia the displacement of the coordinated nitrite by the excess NH_3 was observed leading to formation of the cationic diammine complex $[Mn(TPP)(NH_3)_2]^+$ and free nitrite anion NO_2^-.

Reaction of electron donor ligands with layered **II** results in formation of six-coordinate nitrato-complexes $Mn(TPP)(L)(\eta^1\text{-}ONO_2)$ that display different stabilities depending on the donor strength of L. Although relatively stable in the solid state, these species decompose upon dissolution to yield initial 5-

dx.doi.org/10.1021/ic5014329 | Inorg. Chem. 2014, 53, 11948–11959

coordinate nitrato complex **II**. It is also shown that strong N-donor ligands are able to reversibly display weakly bound nitrate ligand to form bis-ligated cationic complex $[Mn(TPP)(N\text{-donor})_2]^+$ and nitrate anion NO_3^-.

■ ASSOCIATED CONTENT

Supporting Information

FTIR spectrum of $Mn(TPP)(\eta^1\text{-}^{18}O^{15}N^{18}O)$, shifts of porphyrin vibrational modes upon metal oxidation, FTIR spectra of $Mn(TPP)(\eta^1\text{-}ONO_2)$ and $Mn(TPP)(\eta^1\text{-}O^{15}NO_2)$, FTIR spectral changes upon addition of NO_2 to the layered $Mn(TPP)(\eta^1\text{-}O^{15}NO)$, FTIR spectra of $Mn(TPP)(\eta^1\text{-}O^{15}NO)$ and $Mn(TPP)(DMS)(\eta^1\text{-}O^{15}NO)$ at 170 K, FTIR spectra of $Mn(TPP)(THF)(\eta^1\text{-}ONO_2)$ and $Mn(TPP)(THF)(\eta^1\text{-}O^{15}NO_2)$, decomposition of $Mn(TPP)(THF)(\eta^1\text{-}O^{15}NO_2)$ upon dissolution in CCl_4, FTIR spectrum of $Mn(TPP)(DMS)(\eta^1\text{-}ONO_2)$, FTIR spectrum of layered **II** after reaction with NH_3, FTIR spectra of layered **II** after exposure under vapors of Py,FTIR spectral changes upon addition $^{15}NO_2$ on layered $Mn(TPP)(1\text{-}MeIm)(O^{15}NO)$ demonstrating formation of the $Mn(TPP)(1\text{-}MeIm)(O^{15}NO_2)$, and experimental details for obtaining $Mn(TPP)(1\text{-}MeIm)(\eta^1\text{-}ONO_2)$. This material is available free of charge via the Internet at http://pubs.acs.org.

■ AUTHOR INFORMATION

Corresponding Authors

*E-mail. kurto@netsys.am>.

*E-mail. ford@chem.ucsb.edu.

Notes

The authors declare no competing financial interest.

■ ACKNOWLEDGMENTS

This work was supported by the SCS RA (Project No. 13-1D033) and NSF (Project No. CHE-1058794).

■ REFERENCES

(1) (a) Shiva, S.; Sack, M. N.; Greer, J. J.; Duranski, M.; Ringwood, L. A.; Burwell, L.; Wang, X.; MacArthur, P. H.; Shoja, A.; Raghavachari, N.; Calvert, J. W.; Brookes, P. S.; Lefer, D. J.; Gladwin, M. T. *J. Exp. Med.* **2007**, *204*, 2089−2102. (b) Cosby, K.; Partovi, K. S.; Crawford, J. H.; Patel, R. P.; Reiter, C. D.; Martyr, S.; Yang, B. K.; Waclawiw, M. A.; Zalos, G.; Xu, X.; Huang, K. T.; Shields, H.; Kim-Shapiro, D. B.; Schechter, A. N.; Cannon, R. O.; Gladwin, M. T. *Nat. Med.* **2003**, *9*, 1498. (c) Fernandez, B. O.; Bryan, N. S.; Garcia-Saura, M. F.; Bauer, S.; Whitlock, D. R.; Ford, P. C.; Janero, D. R.; Rodriguez, J.; Ashrafian, H. *J. Biol. Chem.* **2008**, *283*, 33927−34. (d) Luchsinger, B. P.; Rich, E. N.; Yan, Y.; Williams, E. M.; Stamler, J. S.; Singel, D. J. *J. Inorg. Biochem.* **2005**, *99*, 912−921.

(2) (a) Gladwin, M. T.; Grubina, R.; Doyle, M. P. *Acc. Chem. Res.* **2009**, *42*, 157−167. (b) Ford, P. C. *Inorg. Chem.* **2010**, *49*, 6226−6239. and references therein (c) Averill, B. A. *Chem. Rev.* **1996**, *96*, 2951−2964.

(3) (a) Silaghi-Dumitrescu, R. *Inorg. Chem.* **2004**, *43*, 3715−3718. (b) Novozhilova, I. V.; Coppens, P.; Lee, J.; Richter-Addo, G. B.; Bagley, K. A. *J. Am. Chem. Soc.* **2006**, *128*, 2093−2104. (c) Kurtikyan, T. S.; Hovhannisyan, A. A.; Hakobyan, M. E.; Patterson, J. C.; Iretskii, A.; Ford, P. C. *J. Am. Chem. Socs* **2007**, *129*, 3576−3585.

(4) (a) Kurtikyan, T. S.; Ford, P. C. *Angew. Chem., Int. Ed.* **2006**, *45*, 492−496. (b) Kurtikyan, T. S.; Hovhannisyan, A. A.; Gulyan, G. M.; Ford, P. C. *Inorg. Chem.* **2007**, *46*, 7024−7031.

(5) (a) Williams, P. A.; Fulop, V.; Garman, E. F.; Saunders, N. F. W.; Ferguson, S. J.; Hajdu, J. *Nature* **1997**, *389*, 406−412. (b) Crane, B. R.; Siegel, M. D.; Getzoff, E. D. *Biochemistry* **1997**, *36*, 12120−12137. (c) Einsle, O.; Messerschmidt, A.; Huber, R.; Kroneck, P. M. J.; Neese, F. *J. Am. Chem. Soc.* **2002**, *124*, 11737−11745.

(6) (a) Copeland, D. M.; Soares, A. S.; West, A. H.; Richter-Addo, G. B. *J. Inorg. Biochem.* **2006**, *100*, 1413−1425. (b) Yi, J.; Safo, M. K.; Richter-Addo, G. B. *Biochemistry* **2008**, *47*, 8247−8249.

(7) Yi, J.; Heinecke, J.; Tan, H.; Ford, P. C.; Richter-Addo, G. B. *J. Am. Chem. Soc.* **2009**, *131*, 18119−18128.

(8) Suslick, K. S.; Watson, R. A. *Inorg. Chem.* **1991**, *30*, 912−919.

(9) Heinecke, J. L.; Yi, J.; Pereira, J. C. M.; Richter-Addo, G. B.; Ford, P. C. *J. Inorg. Biochem.* **2012**, *107*, 47−53.

(10) (a) Olson, J. S.; Foley, E. W.; Rogge, C.; Tsai, A. L.; Doyle, M. P.; Lemon, D. D. *Free Radical Biol. Med.* **2004**, *36*, 685−697. (b) Lundberg, J. O.; Weitzberg, E.; Gladwin, M. T. *Nat. Rev. Drug Discovery* **2008**, *7*, 156−167. (c) Schopfer, M. P.; Wang, J.; Karlin, K. D. *Inorg. Chem.* **2010**, *49*, 6267−6282. (d) Kurtikyan, T. S.; Ford, P. C. *Chem. Commun.* **2010**, *46*, 8570−8572. (e) Su, J.; Groves, J. T. *Inorg. Chem.* **2010**, *49*, 6317−6329. (f) Yukl, E. T.; de Vries, S.; Moenne-Loccoz, P. *J. Am. Chem. Soc.* **2009**, *131*, 7234−7236. (g) Goldstein, S.; Merenyi, G.; Samuni, A. *J. Am. Chem. Soc.* **2004**, *126*, 15694−15701.

(11) Phillippi, M. A.; Baenziger, N.; Goff, H. M. *Inorg. Chem.* **1981**, *20*, 3904−3911. (b) Wyllie, G. R. A.; Munro, O. Q.; Schulz, Ch. E.; Scheidt, W. R. *Polyhedron* **2007**, *26*, 4664−4672.

(12) (a) Kurtikyan, T. S.; Martirosyan, G. G.; Hakobyan, M. E.; Ford, P. C. *Chem. Commun.* **2003**, 1706−1707. (b) Gulyan, G. M.; Kurtikyan, T. S.; Ford, P. C. *Inorg. Chem.* **2008**, *47*, 787−789.

(13) (a) Kurtikyan, T. S.; Eksuzyan, S. R.; Hayrapetyan, V. A.; Martirosyan, G. G.; Hovhannisyan, G. S.; Goodwin, J. A. *J. Am. Chem. Soc.* **2012**, *134*, 13861−13870. (b) Kurtikyan, T. S.; Eksuzyan, S. R.; Goodwin, J. A.; Hovhannisyan, G. S. *Inorg. Chem.* **2013**, *52*, 12046−12056.

(14) Hayashi, T. In *Handbook of Porphyrin Science*; Kadish, K., Smith, K., Guilard, R., Eds.; World Publishing Company: Singapore, 2010; Vol. *5*, Chapter 23, p 2.

(15) Kobayashi, H.; Yanagawa, Y. *Bull. Chem. Soc. Jpn.* **1972**, *45*, 450−454.

(16) (a) Kurtikyan, T. S.; Gasparyan, A. V.; Martirosyan, G. G.; Zhamkochyan, G. A. *J. Appl. Spectrosc.* **1995**, *62*, 62−65. (b) Kurtikyan, T. S.; Ford, P. C. *Coord. Chem. Rev.* **2008**, *252*, 1486−1496. (c) Kurtikyan, T. S.; Gulyan, G. M.; Martirosyan, G. G.; Lim, M. D.; Ford, P. C. *J. Am. Chem. Soc.* **2005**, *127*, 6216−6224. (d) Fateley, W. G.; Bent, H. A.; Crawford, B. *J. Chem. Phys.* **1959**, *31*, 204−217. (e) Lee, C.-I.; Lee, Y.-P.; Wang, X.; Qin, Q.-Z. *J. Chem. Phys.* **1998**, *109*, 10446−10455.

(17) Kurtikyan, T. S.; Stepanyan, T. H.; Martirosyan, G. G.; Kazaryan, R. K.; Madakyan, V. N. *Russ. J. Coord. Chem.* **2000**, *26*, 345−348.

(18) Nakamoto, K. *Infrared and Raman Spectra of Inorganic and Coordination Compounds*, 3rd ed.; Wiley: New York, 1978; p 244.

(19) Paulat, F.; Praneeth, V. K. K.; Nather, C.; Lehnert, N. *Inorg. Chem.* **2006**, *45*, 2835−2856.

(20) (a) Gonzales, B.; Kouba, G.; Yee, S.; Reed, C. A.; Kirner, J. F.; Scheidt, W. R. *J. Am. Chem. Soc.* **1975**, *97*, 3247−3249. (b) Kirner, J. F.; Reed, C. A.; Scheidt, W. R. *J. Am. Chem. Soc.* **1977**, *99*, 1093−1101.

(21) (a) Kurtikyan, T. S.; Stepanyan, T. G.; Akopyan, M. E. *Russ. J. Coord. Chem.* **1999**, *25*, 721−725. (b) Kurtikyan, T. S.; Hovhannisyan, A. A.; Hakobyan, M. E.; Patterson, J. C.; Iretskii, A.; Ford, P. C. *J. Am. Chem. Soc.* **2007**, *129*, 3576−3585.

(22) (a) Kurtikyan, T. S.; Stepanyan, T. G.; Gasparyan, A. V. *Russ. J. Coord. Chem.* **1997**, *23*, 563−567. (b) Kurtikyan, T. S.; Stepanyan, T. G. *Russ. Chem. Bull.* **1998**, *47*, 695−698.

(23) (a) Kurtikyan, T. S.; Hovhannisyan, A. A.; Iretskii, A.; Ford, P. C. *Aust. J. Chem.* **2009**, *62*, 1226−1230. (b) Kurtikyan, T. S.; Hovhannisyan, A. A.; Iretskii, A.; Ford, P. C. *Inorg. Chem.* **2009**, *48*, 11236−11241.

(24) (a) Stepanyan, T. G.; Akopyan, M. E.; Kurtikyan, T. S. *Russ. J. Coor. Chem.* **2000**, *26*, 425−428. (b) Kurtikyan, T. S.; Gulyan, G. M.; Dalaloyan, A. M.; Kidd, B. E.; Goodwin, J. A. *Inorg.Chem.* **2010**, *49*, 7793−98. (c) Kurtikyan, T. S.; Mardyukov, A. N.; Goodwin, J. A. *Russ. J. Coord. Chem.* **2008**, *34*, 606−611.

(25) (a) The pK_a values of the conjugate acids for Py, 1-MeIm, and NH_3 are equal to 5.25, 6.95, and 9.25 correspondingly.[25b] (b) *Hand-*

book of Chemistry and Physics, 77th ed.; Lide, D. A., Ed.; CRC Press: Boca Raton, FL, 1996; Chapter 8, pp 45−55.
(26) Elliot, M. G.; Shepherd, R. E. *Inorg. Chem.* **1987**, *26*, 2067−2073.
(27) Goebbert, D. J.; Garand, E.; Wende, T.; Bergman, R.; Meijer, G.; Asmis, K. R.; Neumark, D. M. *J. Phys. Chem. A* **2009**, *113*, 7584−7592.
(28) (a) Scheidt, R. W. *J. Porphyrins Phthalocyanines* **2008**, *12*, 979−992. (b) Steffen, W. L.; Chun, H. K.; Hoard, J. L.; Reed, C. A. *Abstracts of Papers, 175th National Meeting of the American Chemical Society*, Anaheim, CA, March 13, 1978; American Chemical Society: Washington, D. C., 1978; INOR 15.